Protective effect of luteolin against oxidative stress-mediated cell injury via enhancing antioxidant systems

PINCHA DEVAGE SAMEERA MADUSHAN FERNANDO*, DONG OK KO*, MEI JING PIAO, KYOUNG AH KANG, HERATH MUDIYANSELAGE UDARI LAKMINI HERATH and JIN WON HYUN

Department of Biochemistry, College of Medicine, and Jeju Research Center for Natural Medicine, Jeju National University, Jeju 63243, Republic of Korea

Received November 21, 2023; Accepted April 9, 2024

DOI: 10.3892/mmr.2024.13244

Abstract. Physiological stress such as excessive reactive oxygen species (ROS) production may contribute normal fibroblasts activation into cancer-associated fibroblasts, which serve a crucial role in certain types of cancer such as pancreatic, breast, liver and lung cancer. The present study aimed to examine the cytoprotective effects of luteolin (3',4',5,7-tetrahydroxyflavone) against hydrogen peroxide (H_2O_2)-generated oxidative stress in lung fibroblasts. To examine the effects of luteolin against H_2O_2-induced damages, cell viability, sub-G_1 cell population, nuclear staining with Hoechst 33342, lipid peroxidation and comet assays were performed. To evaluate the effects of luteolin on the protein expression level of apoptosis, western blot assay was performed. To assess the antioxidant effects of luteolin, detection of ROS using H_2DCFDA staining, O_2^- and ·OH using electron spin resonance spectrometer and antioxidant enzyme activity was performed. In a cell-free chemical system, luteolin scavenges superoxide anion and hydroxyl radical generated by xanthine/xanthine oxidase and the Fenton reaction ($FeSO_4/H_2O_2$). Furthermore, Chinese hamster lung fibroblasts (V79-4) treated with H_2O_2 showed a significant increase in cellular ROS. Intracellular ROS levels and damage to cellular components such as lipids and DNA in H_2O_2-treated cells were significantly decreased by luteolin pretreatment. Luteolin increased cell viability, which was impaired following H_2O_2 treatment and prevented H_2O_2-mediated apoptosis. Luteolin suppressed active caspase-9 and caspase-3 levels while increasing Bcl-2 expression and decreasing Bax protein levels. Additionally, luteolin restored levels of glutathione that was reduced in response to H_2O_2. Moreover, luteolin enhanced the activity and protein expressions of superoxide dismutase, catalase, glutathione peroxidase, and heme oxygenase-1. Overall, these results indicated that luteolin inhibits H_2O_2-mediated cellular damage by upregulating antioxidant enzymes.

Introduction

Reactive oxygen species (ROS), such as superoxide anion (O_2^-), hydroxyl radical (·OH), and hydrogen peroxide (H_2O_2), are natural byproducts of oxygen metabolism that serve key roles in cell proliferation and immune responses (1,2). Excessive ROS can damage cellular molecules, leading to DNA damage, lipid peroxidation and protein oxidation. These processes are key in the development of various diseases, including cancer and lung fibrosis (3-5). Cells contain a range of antioxidant enzymes, including superoxide dismutase (SOD), catalase (CAT), and glutathione peroxidase (GPx) and non-enzymatic antioxidants, such as reduced glutathione (GSH), for defense against ROS (6,7). SOD, a metalloenzyme, catalyzes the conversion of O_2^- to molecular O_2 and H_2O_2 and functions as a key component of the cellular antioxidant defense mechanism (8). CAT breaks H_2O_2 into O_2 and H_2O and GPx uses GSH as an electron donor to convert H_2O_2 into its corresponding alcohol or water (9,10). In addition, heme oxygenase-1 (HO-1) serves as a catalyst for the oxidative transformation of heme to carbon monoxide, iron and biliverdin, which is then transformed into bilirubin by biliverdin reductase (11). Furthermore, ROS levels are notably boosted by exposure to environmental stressors, such as ultraviolet light, pollutants and heavy metals (12).

Lung fibroblasts serve a major role in lung development, such as alveolar unit development, aid production of extracellular matrix, and facilitate wound healing and tissue repair (13). Physiological stresses (ROS and disrupted metabolism) may turn normal fibroblasts into cancer-associated fibroblasts (CAFs) (14). CAFs are key factors in the tumor microenvironment and serve a crucial role in non-small cell lung cancer drug resistance (15). Therefore, the present study aimed to identify a potent antioxidant compound capable of ameliorating oxidative stress-mediated cellular defects in fibroblasts.

Luteolin (3',4',5,7-tetrahydroxyflavone) is a flavonoid found abundantly in vegetables and fruits, including green pepper

Correspondence to: Professor Jin Won Hyun, Department of Biochemistry, College of Medicine, and Jeju Research Center for Natural Medicine, Jeju National University, 102 Jeju Daehak, Jeju 63243, Republic of Korea
E-mail: jinwonh@jejunu.ac.kr

*Contributed equally

Key words: luteolin, lung fibroblast, apoptosis, oxidative stress, antioxidant enzyme

and chamomile tea (16). It exhibits antitumor effects against gastric, ovarian, and hepatocellular carcinomas (17-20). Luteolin also possesses numerous biological benefits, such as anti-inflammatory, anti-allergic, and antioxidant properties (21). Given its wide range of therapeutic potentials, the present study aimed to evaluate cytoprotective effects of luteolin on lung fibroblasts via the initiation of antioxidant enzyme activity.

Materials and methods

Reagents and antibodies. Luteolin, 5,5-dimethyl-1-pyrroline-N-oxide (DMPO), xanthine, xanthine oxidase, 2',7'-dichlorodihydrofluorescein diacetate (H_2DCFDA), MTT, thiobarbituric acid (TBA), Hoechst 33342, N-acetyl cysteine (NAC), and propidium iodide (PI) were obtained from Sigma-Aldrich (Merck KGaA). Additionally, 7-amino-4-chloromethylcoumarin (CMAC) and diphenyl-1-pyrenylphosphine (DPPP) were purchased from Molecular Probes (Thermo Fisher Scientific, Inc.) The primary Bax, Bcl-2, GPx, CAT and HO-1 antibodies were obtained from Santa Cruz Biotechnology, Inc.; primary β-actin, phosphorylated (phospho)-H2A histone family member X (H2A.X), H2A.X, caspase-3 and caspase-9 antibodies were obtained from Cell Signaling Technology, Inc.; primary γ-glutamylcysteine ligase (γ-GCL) antibody was obtained from Thermo Fisher Scientific, Inc.; primary Cu/Zn SOD was obtained from Enzo Life Science.

Cell culture. Chinese hamster lung fibroblasts (V79-4) were purchased from American Type Culture Collection and cultured in Dulbecco's modified Eagle medium (Gibco; Thermo Fisher Scientific, Inc.), supplemented with 10% heat-inactivated fetal calf serum, at 37˚C in a humidified incubator with 5% CO_2.

MTT assay. Cells ($1.5x10^5$ cells/ml) were treated with 0.625, 1.250, 2.500, 5.000 or 10.000 μg/ml luteolin for 24 h at 37˚C. To investigate the cytoprotective effect of luteolin against H_2O_2 exposure, cells were pretreated with 2.5 μg/ml luteolin for 1 h before exposure to 1 mM H_2O_2 for 24 h, all at 37˚C. The MTT assay was performed and formazan crystals were dissolved in dimethyl sulfoxide, then absorbance was measured using a scanning multi-well spectrophotometer at 540 nm, as previously described (22).

Evaluation of ROS levels. Cells were exposed to luteolin (0.625, 1.250, 2.500, 5.000 or 10.000 μg/ml, respectively) and 2 mM NAC for 30 min, followed by 1 mM H_2O_2 treatment for 1 h, all at 37˚C. Following staining with 25 μM H_2DCFDA at 37˚C for 10 min, the fluorescence was monitored and quantified using a spectrofluorometer (PerkinElmer FL 6500 Fluorescence Spectrometer with Spectrum FL Software 1.1 version, PerkinElmer Inc.) or a confocal microscope (Zeiss LSM 510 confocal microscope with Zen 2.5 version, Carl Zeiss Inc.), as previously described (23) using 40x magnification.

Detection of superoxide anion. The xanthine/xanthine oxidase system was used to produce O_2^-, which was captured by the nitrone spin trap, DMPO. The resulting DMPO/·OOH adducts were identified using electron spin resonance (ESR) spectrometer (JEOL, Ltd.) as previously described (23).

Detection of hydroxyl radical. Hydroxyl radical was generated by the Fenton reaction (H_2O_2 + $FeSO_4$) and detected by capturing with DMPO to form DMPO/·OH adducts, measured using ESR spectrometer as previously described (23).

Assessment of lipid peroxidation. Following cell treatment with 5 μM DPPP at 37˚C for 30 min, a fluorescence microscope (Zeiss LSM 510 confocal microscope with Zen 2.5 version; 20x magnification) was used to assess images of DPPP fluorescence. The cells were rinsed with cold PBS, scraped and homogenized in ice-cold 1.15% KCl, resulted cell lysate was subjected to further assessment. For the detection of TBA reactive substances (TBARS), 100 μl cell lysates were mixed with 0.2 ml sodium dodecyl sulfate (SDS, 8.1%), 1.5 ml 20% acetic acid (pH 3.5) and 1.5 ml TBA (0.8%) and combined with 5 ml 15:1 (v/v) n-butanol and pyridine solutions. The resulting supernatant absorbance was measured using a spectrophotometer at 532 nm.

Comet assay. Following treatment with luteolin and H_2O_2, cells were collected and centrifuged at 15,000 x g for 5 min, following washing with PBS to obtain cell pellets. Cell pellets on 1% agarose-coated slides were subjected to gel electrophoresis at 300 mA and 25 V for 20 min in darkness at 20˚C. Ethidium bromide (20 μg/ml) stained slides at 20˚C for 5 min were examined under a fluorescence microscope (Komet 7 with Zyla 5.5 USB 3.0 sCMOS camera, Andor Technology; 20x magnification). Each slide contained 50 cells and data on tail length and total fluorescence percentages were analyzed using Komet version 5.5 image analyzer software (Andor Technology).

Western blot analysis. Total proteins from the cells was extract by using PRO-PREP™ protein extraction solution (iNtRON Biotechnology). Thereafter total protein levels were estimated by protein assay reagent kit (Bio-Rad). A total of 30 μg/lane cell lysates were subjected to electrophoresis on a 10% SDS-polyacrylamide gel, transferred to nitrocellulose membranes, subjected for blocking with 3% bovine serum albumin (Bovogen Biologicals Pty Ltd.) for 1 h at 20˚C, and then incubated with the corresponding primary antibodies whereas phospho-H2A.X (cat. #9718), H2A.X (cat. #2595), β-actin (cat. #4967), Bax (cat. sc-7480), Bcl-2 (cat. sc-7382), caspase-9 (cat. #9508), caspase-3 (cat. #9662), γ-GCL (cat. #RB-1697-P0, -P1), Cu/Zn SOD (cat. ADI-SOD-100), CAT (cat. sc-34285), GPx (cat. sc-22145), HO-1 (cat. sc-10789) (all 1:1,000 ratio, respectively) and for overnight at 4˚C subsequently treated with the relevant secondary (diluted 1:10,000, respectively) goat anti-rabbit IgG (H+L) Secondary antibody, HRP (cat. #31460) and goat anti-mouse IgG (H+L) secondary antibody, HRP (cat. #31430; Thermo Fisher Scientific, Inc.) at 20˚C for 1 h. Each corresponding protein band was observed on an X-ray film following treat with enhanced chemiluminescence western blotting detection kit (Amersham) as previously described (23).

Hoechst 33342 nuclear staining. Cells were stained with Hoechst 33342, a DNA-specific probe, at 37˚C for 10 min. The degree of nuclear condensation was evaluated using a fluorescence microscope (BH2-RFL-T3; Olympus; 20x magnification) fitted with a CoolSNAP-Pro color digital camera (Media Cybernetics) to observe stained cells.

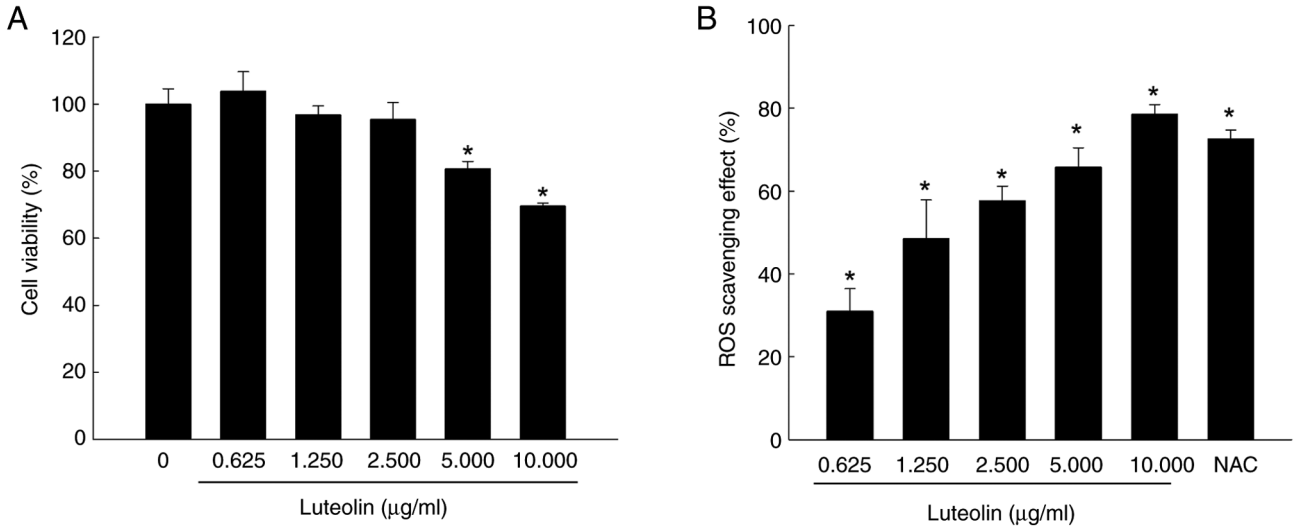

Figure 1. Effect of luteolin on cytotoxicity and ROS scavenging following H_2O_2 treatment. (A) Cells were treated with luteolin for 24 h. Cell viability was determined using the MTT assay. *P<0.05 vs. 0. (B) Cells were pretreated with luteolin, followed by treatment with 1 mM H_2O_2 after 30 min. Following H_2DCFDA treatment, intracellular ROS levels were evaluated by spectrofluorometry. The antioxidant NAC was employed as the positive control. *P<0.05 vs. 0. ROS, reactive oxygen species; NAC, N-acetyl cysteine.

Detection of sub-G_1 cells. Cells were fixed with 70% ethanol at 4˚C for 30 min, subjected for washing with PBS, mixed in 1 ml PBS containing 100 μg PI solution and 100 μg RNase A and incubated in dark conditions at 37˚C for 30 min. The percentage of apoptotic sub-G_1 cells was determined using FACSCalibur flow cytometer with CellQuest pro software 4.02 (Becton Dickinson).

GSH detection. Cells were incubated with 5 μM CMAC at 37˚C, a GSH-sensitive fluorescent dye, for 30 min. Images of CMAC fluorescence in response to GSH were analyzed using a fluorescence microscope (BH2-RFL-T3; Olympus; 10x magnification) (23).

Assessment of SOD activity. Collected cells were sonicated twice for 15 sec in 10 mM phosphate buffer (pH 7.5) on ice to lyse. 1% Triton X-100 was added to the lysates and incubated on ice for 10 min. After centrifugation at 5,000 x g for 10 min at 4˚C, the lysates were cleared of debris and the protein concentration of the supernatant was measured utilizing using the Bradford method. Cell lysates were mixed with 500 mM phosphate buffer (pH 10.2) and 1 mM epinephrine at 20˚C, which auto-oxidizes to form adrenochrome, and the reactants were measured at 480 nm using a ultraviolet/visible spectrophotometer in kinetic mode. SOD activity was calculated as unit/mg protein as previously described (23).

Assessment of CAT activity. Harvested cells were suspended in 10 mM phosphate buffer (pH 7.5) and sonicated twice for 15 sec on ice. After adding 1% TritonX-100 to the lysates, they were incubated on ice for 10 min. Protein content was measured after centrifuging lysates at 5,000 x g for 30 min at 4˚C to eliminate cellular debris. Then cell lysates were reacted with 50 mM phosphate buffer (pH 7) and 100 mM H_2O_2, at 37˚C for 2 min. Absorbance changes at 240 nm over 5 min were measured by spectrophotometer (X-ma 1000; Human Corporation) to determine the rate of H_2O_2 decomposition.

Assessment of GPx activity. Cells were lysed by sonicating twice for 15 sec in 10 mM phosphate buffer (pH 7.5) on ice. 1% Triton X-100 was added to lysates and incubated on ice for 10 min. After centrifugation at 5,000 x g for 10 min at 4˚C, debris was removed and protein concentration was assessed using the Bradford technique. Then cell lysates were mixed with 25 mM phosphate buffer (pH 7.5), 1 mM EDTA, NaN_3, GSH, 0.25 units of glutathione reductase, and 0.1 mM NADPH. Following 10 min incubation at 37˚C, 1 mM H_2O_2 was added for 1 min at 37˚C and absorbance was measured using spectrophotometer (X-ma 1000, Human Co.) at 340 nm for 5 min.

Assessment of HO-1 activity. Cells were washed with PBS, collected in PBS (pH 7.4), allowed to 15 min incubation on ice facilitating brief sonication and added sucrose solution obtaining 0.25 M sucrose as final concentration. Homogenates were centrifuged 10 min at 1,000 x g at 4˚C. The supernatants were centrifuged at 12,000 x g for 15 min at 4˚C and afterward at 105,000 x g for 60 min at 4˚C. Resulted pellet was resuspended in 50 mM PBS (pH 7.4) and protein concentration was measured using the Bradford technique. Cell lysates were suspended in a reaction mixture containing 0.2 mM hemin, 0.5 mg/ml rat liver cytosol (supplying biliverdin reductase; Creative Bioarray; cat. no. DDM-M063), 2 mM glucose-6-phosphate, 1 unit/ml glucose-6-phosphate dehydrogenase, 1 mM NADPH and 50 mM PBS (pH 7.4) for 2 h at 37˚C. The chloroform-extracted layer was assessed using a spectrophotometer at 464 and 530 nm.

Statistical analysis. All experiments were performed in triplicate, with results presented as the mean ± standard error. Data were analyzed using one way analysis of variance, followed by Tukey's post hoc test to determine the differences using SigmaStat 3.5 version software (Systat Software Inc.). P<0.05 was considered to indicate a statistically significant difference.

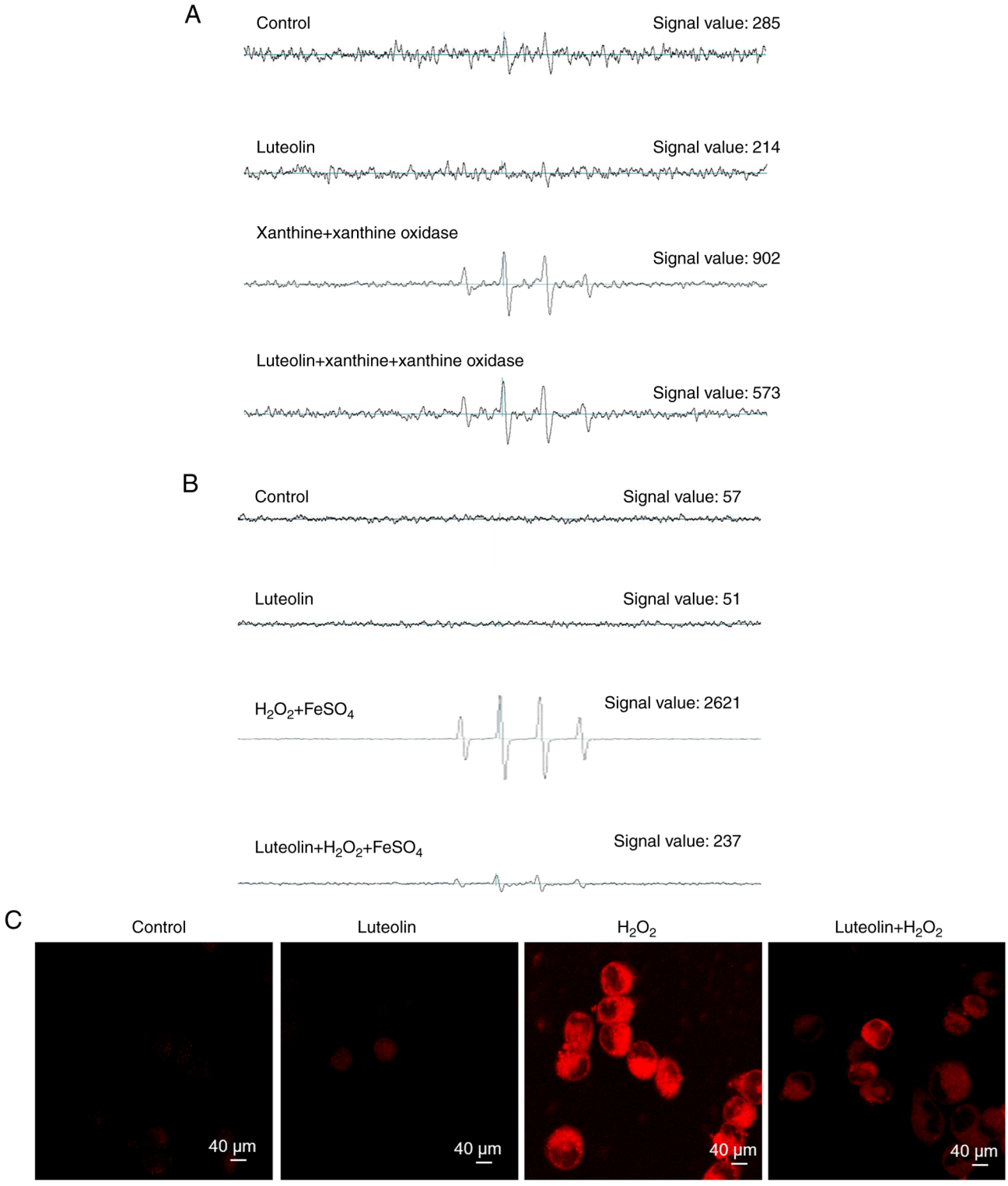

Figure 2. Effect of luteolin on scavenging of superoxide anion, hydroxyl radical and intracellular ROS. (A) Superoxide anion produced through xanthine and xanthine oxidase interacted with DMPO. The resulting DMPO/·OOH adducts were identified via ESR spectrometry. (B) Hydroxyl radical interacted with DMPO and the resulting DMPO/·OH adducts were identified by ESR spectrometry. (C) 2',7'-Dichlorodihydrofluorescein diacetate technique was utilized to estimate intracellular ROS levels. ROS, reactive oxygen species; DMPO, 5,5-dimethyl-1-pyrroline-N-oxide; ESR, electron spin resonance.

Results

Effect of luteolin on ROS scavenging. Luteolin exhibited no cytotoxicity toward V79-4 cells at concentrations of 0.625, 1.25 and 2.5 μg/ml. Cytotoxic effects were observed at concentrations of 5 and 10 μg/ml (Fig. 1A). Fluorescence spectrometry indicated that luteolin scavenged intracellular ROS in a dose-dependent manner, decreasing ROS by 31% at 0.625, 51% at 1.250, 58% at 2.500, 68% at 5.000 and 75% at 10.000 μg/ml (Fig. 1B). The ROS scavenger NAC, serving as a positive control, eliminated 72% of ROS. Given its cell viability and ROS-scavenging ability, 2.5 μg/ml luteolin was selected

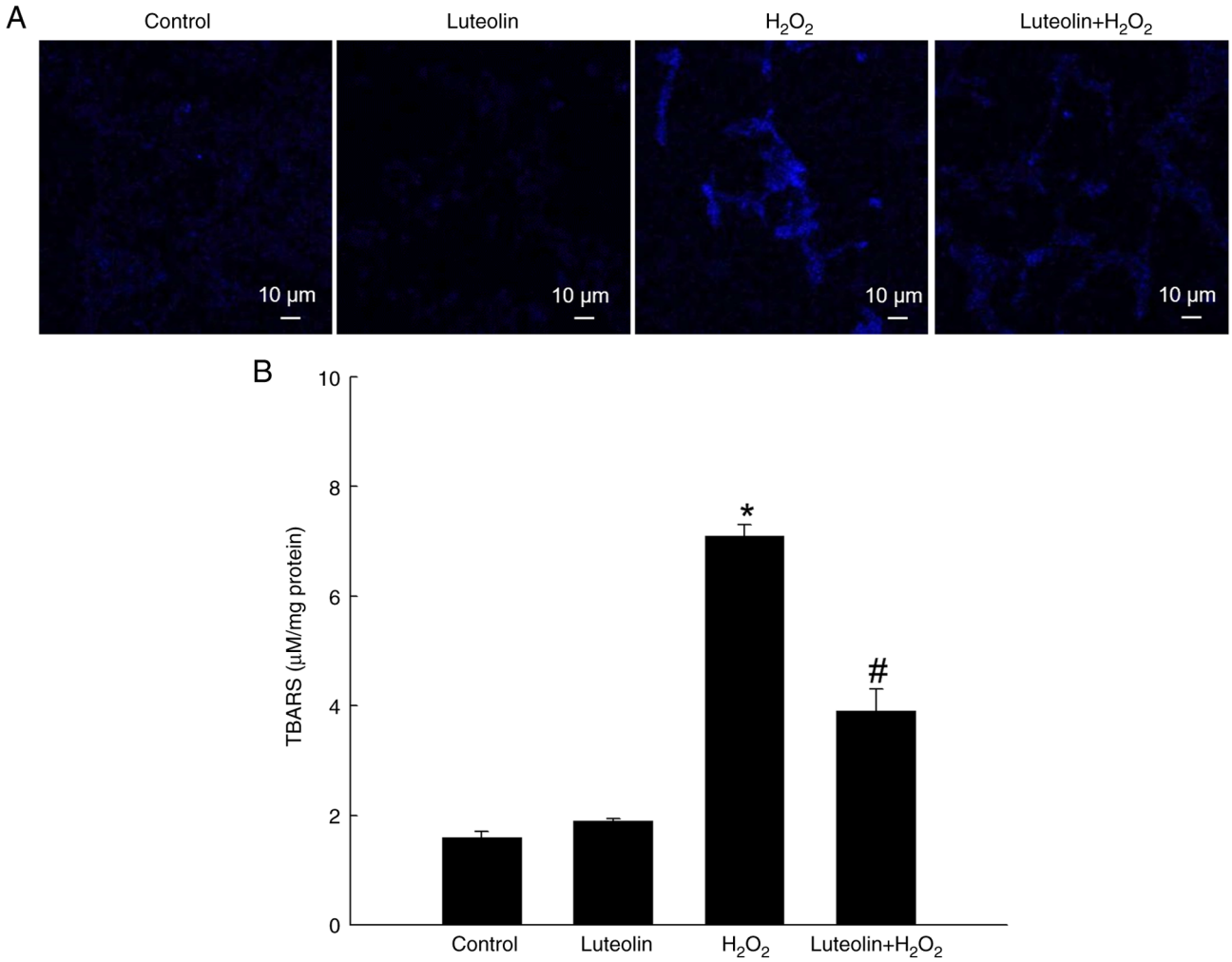

Figure 3. Protective ability of luteolin on H_2O_2-induced cellular lipid peroxidation. Cellular lipid peroxidation was determined via (A) diphenyl-1-pyrenylphosphine staining and (B) TBARS assay. *P<0.05 vs. control; #P<0.05 vs. H_2O_2. TBARS, thiobarbituric acid reactive substances.

as the optimal dose for further evaluation. ESR spectrometry was used to quantify the superoxide anion generated by the xanthine/xanthine oxidase system. ESR measurement revealed an elevation in the superoxide anion signal to 902 in this system. However, when the superoxide anion was treated with luteolin, the superoxide anion signal was reduced to 573, indicating the direct scavenging effect of luteolin on the superoxide anion produced via the xanthine/xanthine oxidase pathway (Fig. 2A). Furthermore, ESR spectrometry was used to detect the hydroxyl radical produced via the Fenton reaction. ESR measurement demonstrated that neither the control nor luteolin at 2.5 μg/ml exhibited a signal, whereas the signal of the hydroxyl radical increased to 2,621 in the Fenton reaction system. Treatment with luteolin markedly decreased the hydroxyl radical signal to 237, indicating the capacity of luteolin to directly mitigate the hydroxyl radical generated through the Fenton reaction system (Fig. 2B). Additionally, confocal microscopy images from the H_2DCFDA assay showed that luteolin suppressed red fluorescence intensity, which increased in response to H_2O_2 treatment in association with elevated ROS levels (Fig. 2C).

Effect of luteolin on H_2O_2-induced lipid peroxidation. The capacity of luteolin to counteract membrane lipid peroxidation in cells exposed to H_2O_2 was assessed. Lipid peroxidation, evidenced by formation of the highly fluorescent compound DPPP oxide upon DPPP stoichiometric reaction with lipid hydroperoxides, was assessed (24). H_2O_2 treatment enhanced DPPP fluorescence intensity, indicating the elevation of lipid peroxidation levels (Fig. 3A). However, this increase was notably attenuated by treatment with 2.5 μg/ml luteolin. Additionally, protective effect of luteolin against lipid peroxidation was demonstrated by TBARS formation in H_2O_2-treated V79-4 cells whereas luteolin significantly decreased H_2O_2-induced TBARS formation (Fig. 3B).

Effect of luteolin against DNA damage. The comet assay, a sensitive technique for measuring DNA damage (25), demonstrated that H_2O_2 resulted in a 77% increase in the length and quantity of DNA in the comet tail, signifying considerable DNA damage; however, pretreatment with luteolin reduced this increase to 51% (Fig. 4A). Furthermore, evaluation of phospho-H2A.X, a marker for DNA double-strand breaks (25), showed that luteolin pretreatment diminished expression levels of phospho-H2A.X in H_2O_2-exposed cells (Fig. 4B). There was no change in total H2A.X expression.

Effect of luteolin on cell survival following H_2O_2 treatment. Pretreatment with 2.5 μg/ml luteolin in conjunction with

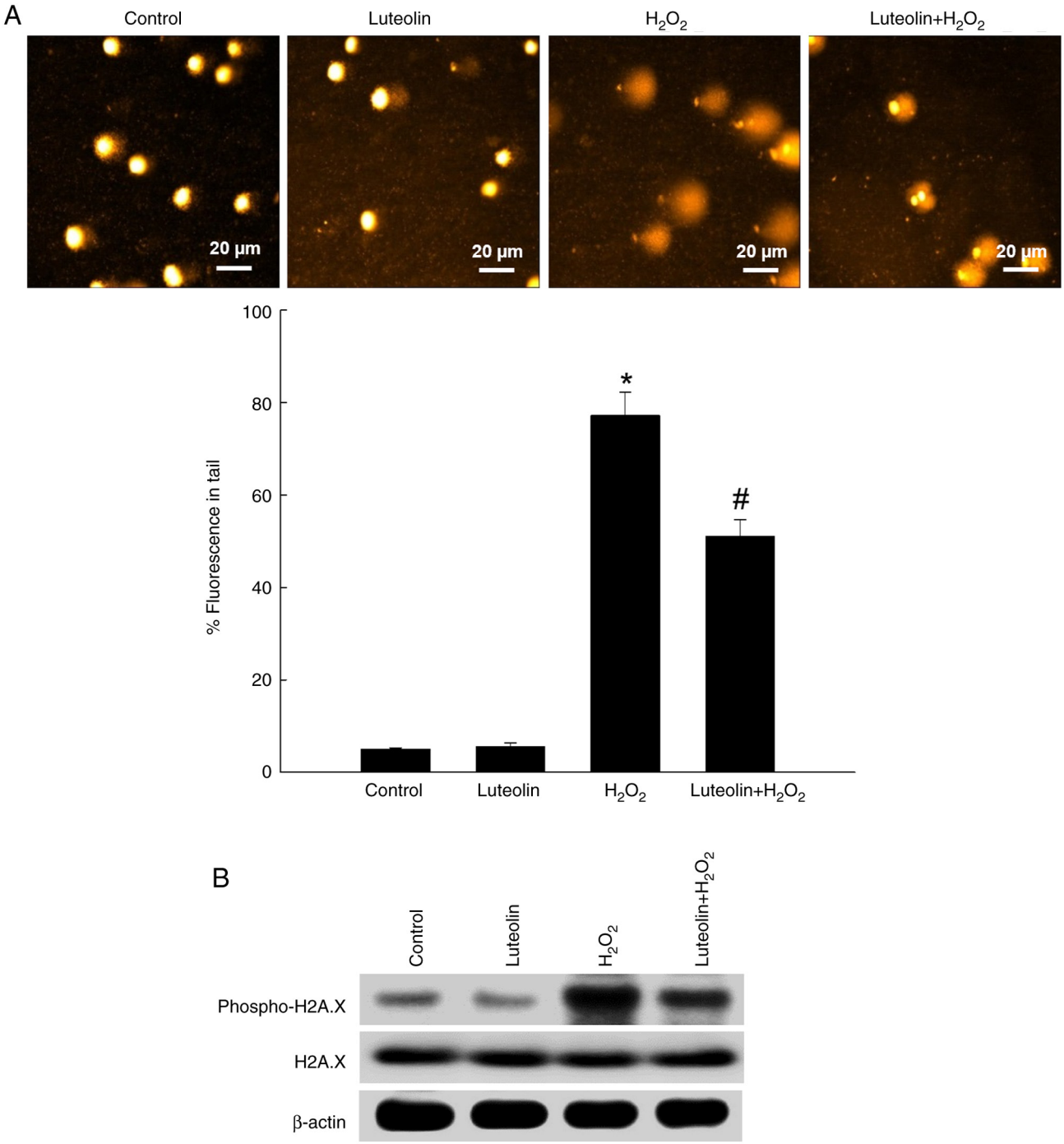

Figure 4. Cytoprotective effect of luteolin on H_2O_2-induced DNA damage. (A) Alkaline comet assay was used for the identification of DNA damage. Representative pictures and cellular DNA damage (% fluorescence in the tail) are presented. *P<0.05 vs. control; #P<0.05 vs. H_2O_2. (B) Western blot analysis with antibody against total and phospho-H2A.X was performed. β-actin was used as the loading control. Phospho-H2A.X, phosphorylated-histone H2A histone family member X.

H_2O_2 significantly increased cell viability to 77% compared with 54% in cells treated solely with H_2O_2 (Fig. 5A). The cytoprotective effect of luteolin against H_2O_2-induced apoptosis was determined by staining nuclei of cells with Hoechst 33342 and observing them under a microscope. H_2O_2-treated cells showed considerable nuclear fragmentation and apoptotic morphology; however, luteolin pretreatment alleviated H_2O_2-induced cellular apoptosis (Fig. 5B). The proportion of sub-G_1 in H_2O_2-treated cells was 33% (a 31% increase relative to the control; Fig. 5C); however, pretreatment with luteolin decreased the sub-G_1 apoptotic cells to 12%. Pretreatment with luteolin led to an alleviation of H_2O_2-induced pro-apoptotic protein Bax expression and increased the anti-apoptotic Bcl-2 protein expression, which was decreased by H_2O_2 (Fig. 5D). Furthermore, luteolin alleviated H_2O_2-mediated activation of caspase-9 and caspase-3 (Fig. 5D).

Effect of luteolin on antioxidant systems. Confocal microscopy showed a notable reduction in GSH level in H_2O_2-treated cells, showing lower fluorescence intensity than that of the

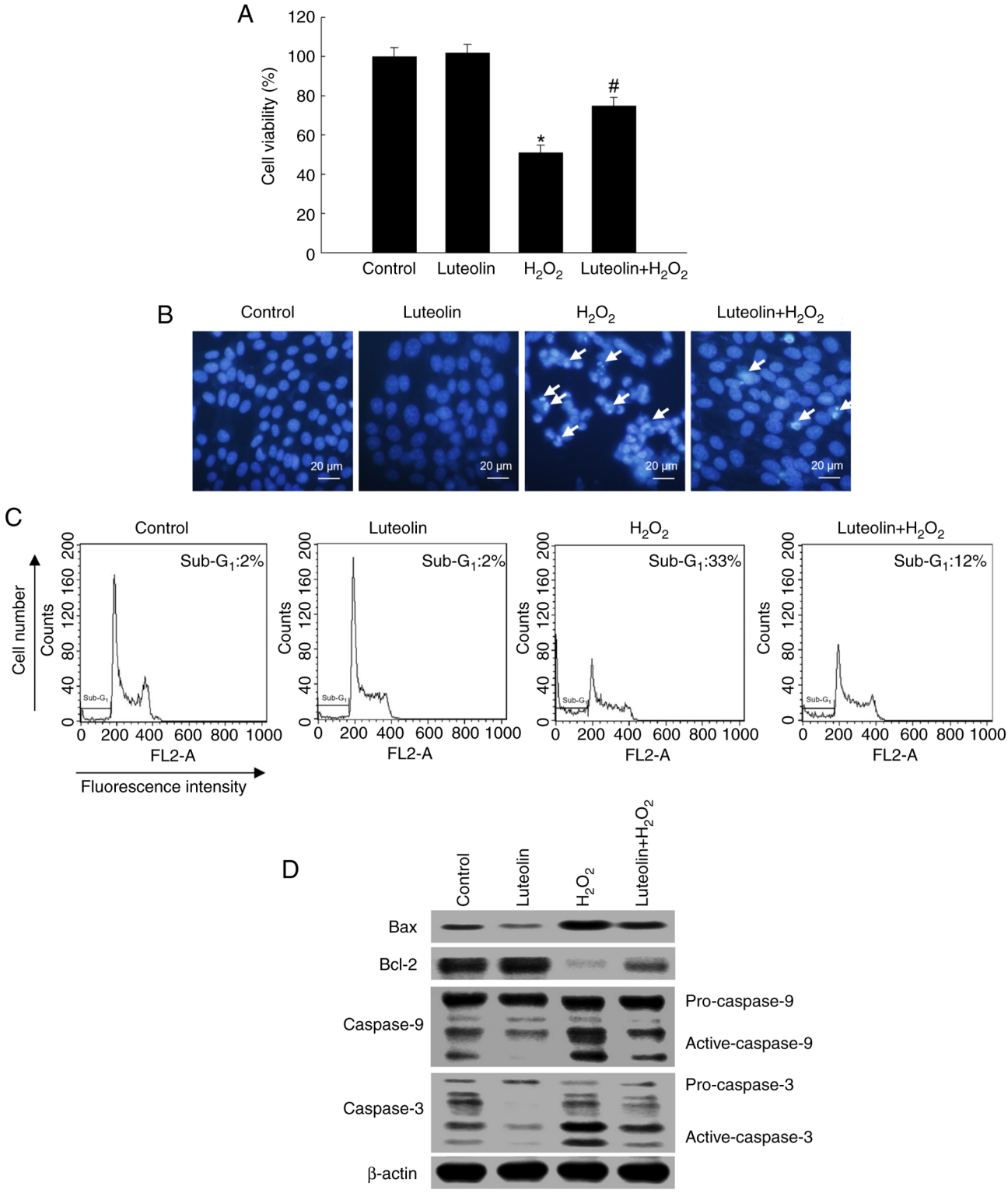

Figure 5. Cytoprotective effect of luteolin on H_2O_2-induced apoptosis. (A) MTT assay was used to assess cell viability. $^*P<0.05$ vs. control; $^\#P<0.05$ vs. H_2O_2. (B) Apoptotic bodies (arrow) were revealed by Hoechst 33342 staining. (C) Sub-G_1 cells, which is indicative of apoptosis, were identified by flow cytometry. (D) Western blot analysis with antibodies against Bax, Bcl-2, active caspase-9 and caspase-3 was performed. β-actin was employed as a loading control.

control. However, an increase in GSH levels was observed in the luteolin-pretreated group (Fig. 6A). As GSH synthesis involves γ-GCL and GSH synthase (26), γ-GCL expression was evaluated via western blotting. The expression of γ-GCL was notably downregulated by H_2O_2-treated cells but upregulated by luteolin pretreatment (Fig. 6B). Moreover, enzymatic assays demonstrated that luteolin pretreatment enhanced activities of SOD, CAT, GPx, and HO-1 to 29, 17 and 17 unit/mg protein and 7,162 pmol bilirubin/mg protein, respectively, compared with diminished activities in cells treated with H_2O_2-alone (23, 9, and 9 unit/mg protein and 4,987 pmol bilirubin/mg protein, respectively; Fig. 6C and D). Also, the levels of SOD, CAT,

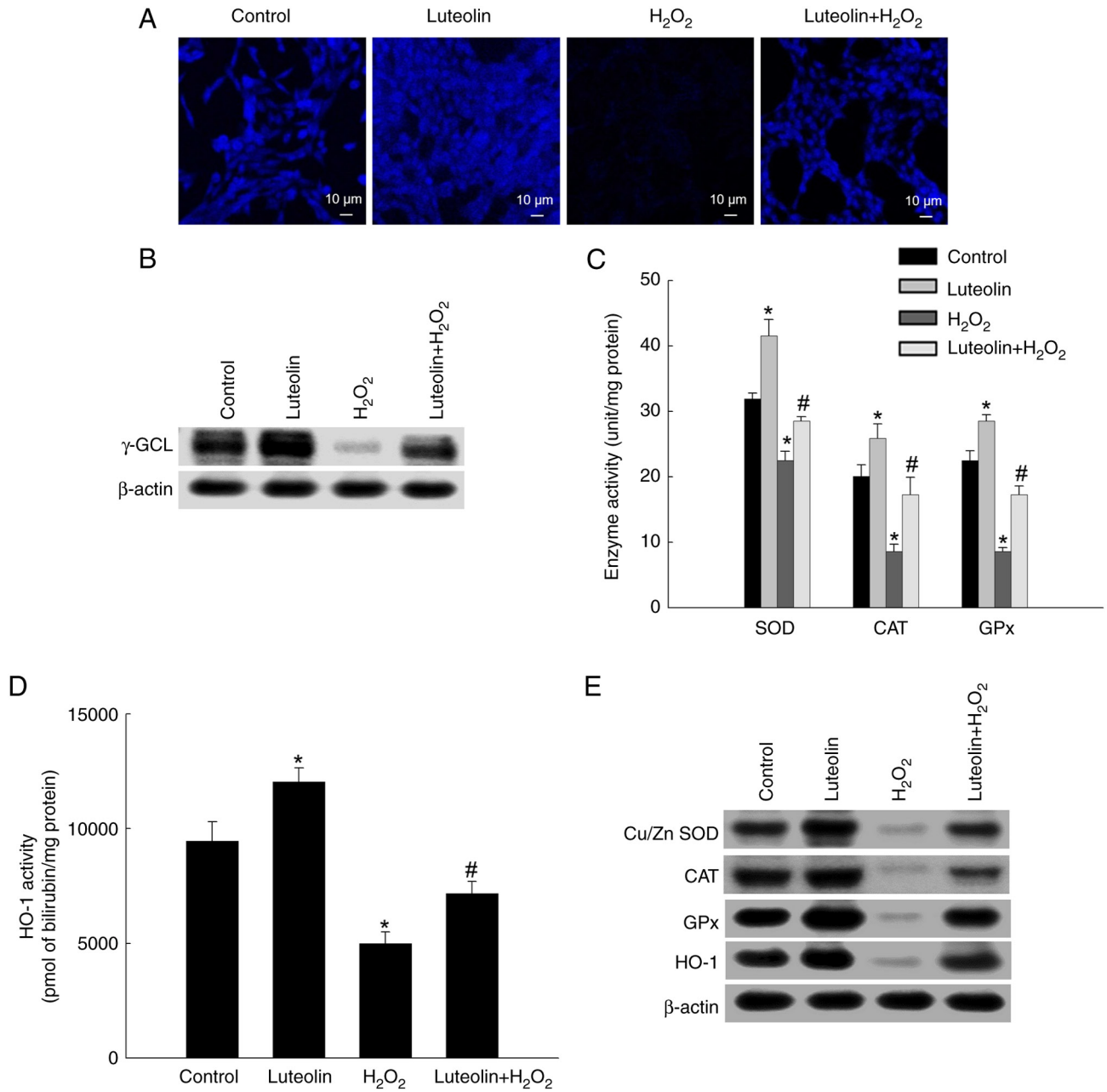

Figure 6. Effect of luteolin on antioxidant systems. (A) 7-Amino-4-chloromethylcoumarin dye was used to detect intracellular GSH levels. (B) Western blot analysis with antibody against γ-GCL was assessed. (C) The activities of SOD, CAT, and GPx were presented as unit per mg of protein. (D) HO-1 enzyme activity was shown as pmol bilirubin/mg protein. (E) Western blotting analysis with antibodies for Cu/Zn SOD, CAT, GPx and HO-1. β-actin was employed as a loading control. *P<0.05 vs. control; #P<0.05 vs. H_2O_2. GSH, glutathione; γ-GCL, γ-glutamylcysteine ligase; SOD, superoxide dismutase; CAT, catalase; GPx, glutathione peroxidase; HO-1, heme oxygenase-1.

GPx and HO-1 were reduced in H_2O_2-treated cells; however, luteolin partially restored expression of these proteins (Fig. 6E).

Discussion

Flavonoids are categorized based on their molecular structures into flavan-3-ols, flavones, flavonols, flavanones, isoflavones, and anthocyanins (27). These substances are abundantly found in coffee, fruit, vegetables and cocoa-containing products (28). Flavonoids are known for broad therapeutic benefits, including anticancer, antioxidant, anti-inflammatory, anti-microbial and antiangiogenic effects (29). Extensive research, including our prior studies, has demonstrated that luteolin induces apoptosis in various types of cancer cells, such as human colon, melanoma, lung, cervical, monocytic leukemia and breast cancer cells (23,30-32). Notably, Liu *et al* (33) reported the protective effects of luteolin against angiotensin II-induced renal damage in apolipoprotein E-deficient mice. The present study evaluated the antioxidant potential of luteolin against H_2O_2-induced oxidative stress in lung fibroblasts and demonstrated that luteolin inhibited H_2O_2-mediated cellular damage by upregulating antioxidant enzymes.

ROS induce cellular damage and cause disease progression, including chronic obstructive pulmonary disease (COPD) and pulmonary fibrosis (34,35). Here, luteolin showed potent

scavenging capabilities for O_2^- and ·OH in a cell-free system. Additionally, pretreatment with luteolin resulted in a significant decrease in intracellular levels of ROS. Given its efficacy in neutralizing ROS, including O_2^- and ·OH, luteolin may serve as a promising therapeutic agent for management and treatment of conditions such as COPD and pulmonary fibrosis.

ROS-induced lipid peroxidation compromises cellular membranes (36). Polyunsaturated fatty acids, particularly those vulnerable to ROS, undergo peroxidation, leading to a cascade of free radical reactions (34,37,38). Here, H_2O_2 strongly promoted lipid peroxidation and TBARS production; however, luteolin inhibited lipid peroxidation in the cell membranes. GPx catalyzes conversion of H_2O_2 into water and lipid peroxides into their corresponding alcohols (6). Moreover, bilirubin, a product of HO-1 activity, offers protection against lipid peroxidation (39). The present study indicates that luteolin directly scavenges ROS and upregulates antioxidant enzymes such as GPx and HO-1, thereby mitigating lipid peroxidation. Additionally, luteolin decreased DNA damage and phospho-H2A.X protein levels that were elevated by H_2O_2 treatment. The present study investigated proteins associated with the mitochondrial cell death pathway to gain insight into the mechanisms of apoptosis as mitochondria-mediated apoptosis can be induced in response to H_2O_2 exposure (40,41). Luteolin suppressed active caspase-9 and caspase-3 while lowering the levels of the pro-apoptotic protein Bax and increasing the levels of anti-apoptotic protein Bcl-2. As luteolin attenuated cellular lipid peroxidation and DNA damage and inhibits H_2O_2-mediated cell apoptosis in the present study, we focused on the antioxidant capacity of luteolin to decrease the adverse effect of H_2O_2.

The cellular antioxidant system, comprising enzymes such as SOD, CAT, GPx, and HO-1, serves a crucial role in mitigating oxidative stress-induced cellular damage (42,43). As evidenced by CMAC staining and western blotting, luteolin pretreatment restored H_2O_2 mitigated GSH and γ-GCL levels. H_2O_2 treatment reduced levels and enzymatic activity of SOD, CAT, GPx, and HO-1 proteins, which were subsequently restored by luteolin pretreatment. Previous research has indicated that luteolin upregulates NRF2 and HO-1 expression, thereby decreasing H_2O_2-induced oxidative damage in intestinal epithelial cells (44). Additionally, luteolin is known to promote autophagy and antioxidant processes via activation of the p62/KEAP1/NRF2 pathway, which has been identified for its neuroprotective effect (45). Luteolin scavenges ROS by enhancing antioxidant enzymes by regulating the NRF2 signaling pathway (46,47). The NRF2 signaling pathway is integral to cellular antioxidant defenses and maintenance of redox homeostasis, regulating the expression of antioxidant and drug-metabolizing enzymes such as SOD, CAT, GPx, and HO-1 (48). The present study demonstrates that luteolin activates these antioxidant enzymes to counteract H_2O_2-induced oxidative stress, suggesting induction of these enzymes via the NRF2 signaling pathway. Taken together, the present results suggested that luteolin can prevent ROS generation by mitigating cellular damage and improving antioxidant enzyme activity.

In conclusion, luteolin inhibited H_2O_2-induced lipid peroxidation, DNA damage, and cell apoptosis while augmenting the activity of cellular antioxidant enzymes (CAT, SOD, GPx, and HO-1), thus safeguarding V79-4 cells from oxidative harm. These properties position luteolin as a potential agent for protecting lung fibroblasts against oxidative damage, warranting further clinical investigation to assess its efficacy in alleviating oxidative stress-associated pulmonary conditions.

Acknowledgements

Not applicable.

Funding

The present study was supported by the National Research Foundation of Korea, funded by the Ministry of Education (grant no. RS-2023-00270936) and the Ministry of Science and ICT (grant no. NRF-2023R1A2C1002770).

Availability of data and materials

All data generated or analyzed during this study are included in this published article.

Authors' contributions

PDSMF, DOK, and JWH conceived and designed the study and wrote the manuscript. DOK, HMULH, MJP, and KAK performed the experiments and data analysis and interpretation. PDSMF and JWH confirm the authenticity of all the raw data. PDSMF, DOK, HMULH, and JWH revised the manuscript for important intellectual content. All authors have read and approved the final manuscript.

Ethics approval and consent to participate

Not applicable.

Patient consent for publication

Not applicable.

Competing interests

The authors declare that they have no competing interests.

Reference

1. Shah S, Sun A and Chu XP: Modulation of ASIC1a by reactive oxygen species through JFK signaling. Int J Physiol Pathophysiol Pharmacol 14: 276-280, 2022.
2. Banerjee S, Ghosh S, Mandal A, Ghosh N and Sil PC: ROS-associated immune response and metabolism: A mechanistic approach with implication of various diseases. Arch Toxicol 94: 2293-2317, 2020.
3. Meher PK and Mishra KP: Radiation oxidative stress in cancer induction and prevention. J Radiat Cancer Res 8: 44-52, 2017.
4. Martins SG, Zilhão R, Thorsteinsdóttir S and Carlos AR: Linking oxidative stress and DNA damage to changes in the expression of extracellular matrix components. Front Genet 12: 673002, 2021.
5. Sakai T, Takagaki H, Yamagiwa N, Ui M, Hatta S and Imai J: Effects of the cytoplasm and mitochondrial specific hydroxyl radical scavengers TA293 and mitoTA293 in bleomycin-induced pulmonary fibrosis model mice. Antioxidants (Basel) 10: 1398, 2021.
6. Ighodaro OM and Akinloye OA: First line defence antioxidants-superoxide dismutase (SOD), catalase (CAT) and glutathione peroxidase (GPX): Their fundamental role in the entire antioxidant defence grid. Alexandria J Med 54: 287-293, 2018.

7. Averill-Bates DA: The antioxidant glutathione. Vitam Horm 121: 109-141, 2023.
8. Saxena P, Selvaraj K, Khare SK and Chaudhary N: Superoxide dismutase as multipotent therapeutic antioxidant enzyme: Role in human diseases. Biotechnol Lett 44: 1-22, 2022.
9. Kaushal J, Mehandia S, Singh G, Raina A and Arya SK: Catalase enzyme: Application in bioremediation and food industry. Biocatal Agric Biotechnol 16: 192-199, 2018.
10. Sharapov MG, Gudkov SV and Lankin VZ: Hydroperoxide-reducing enzymes in the regulation of free-radical processes. Biochemistry (Mosc) 86: 1256-1274, 2021.
11. Ryter SW: Therapeutic potential of heme oxygenase-1 and carbon monoxide in acute organ injury, critical illness, and inflammatory disorders. Antioxidants (Basel) 9: 1153, 2020.
12. Pizzino G, Irrera N, Cucinotta M, Pallio G, Mannino F, Arcoraci V, Squadrito F, Altavilla D and Bitto A: Oxidative stress: Harms and benefits for human health. Oxid Med Cell Longev 2017: 8416763, 2017.
13. Nova Z, Skovierova H and Calkovska A: Alveolar-capillary membrane-related pulmonary cells as a target in endotoxin-induced acute lung injury. Int J Mol 20: 831, 2019.
14. Sahai E, Astsaturov I, Cukierman E, DeNardo DG, Egeblad M, Evans RM, Fearon D, Greten FR, Hingorani SR, Hunter T, *et al*: A framework for advancing our understanding of cancer-associated fibroblasts. Nat Rev Cancer 20: 174-186, 2020.
15. Chen C, Hou J, Yu S, Li W, Wang X, Sun H, Qin T, Claret FX, Guo H and Liu Z: Role of cancer-associated fibroblasts in the resistance to antitumor therapy, and their potential therapeutic mechanisms in non-small cell lung cancer. Oncol Lett 21: 413, 2021.
16. Tan X, Liu B, Lu J, Li S, Baiyun R, Lv Y, Lu Q and Zhang Z: Dietary luteolin protects against HgCl2-induced renal injury via activation of Nrf2-mediated signaling in rat. J Inorg Biochem 179: 24-31, 2018.
17. Lu J, Li G, He K, Jiang W, Xu C, Li Z, Wang H, Wang W, Wang H, Teng X and Teng L: Luteolin exerts a marked antitumor effect in cMet-overexpressing patient-derived tumor xenograft models of gastric cancer. J Transl Med 13: 42, 2015.
18. Wang H, Luo Y, Qiao T, Wu Z and Huang Z: Luteolin sensitizes the antitumor effect of cisplatin in drug-resistant ovarian cancer via induction of apoptosis and inhibition of cell migration and invasion. J Ovarian Res 11: 93, 2018.
19. Yu Q, Zhang M, Ying Q, Xie X, Yue S, Tong B, Wei Q, Bai Z and Ma L: Decrease of AIM2 mediated by luteolin contributes to non-small cell lung cancer treatment. Cell Death Dis 10: 218, 2019.
20. Xu H, Yang T, Liu X, Tian Y, Chen X, Yuan R, Su S, Lin X and Du G: Luteolin synergizes the antitumor effects of 5-fluorouracil against human hepatocellular carcinoma cells through apoptosis induction and metabolism. Life Sci 144: 138-147, 2016.
21. Imran M, Rauf A, Abu-Izneid T, Nadeem M, Shariati MA, Khan IA, Imran A, Orhan IE, Rizwan M, Atif M, *et al*: Luteolin, a flavonoid, as an anticancer agent: A review. Biomed Pharmacother 112: 108612, 2019.
22. Fernando PDSM, Piao MJ, Zhen AX, Ahn MJ, Yi JM, Choi YH and Hyun JW: Extract of cornus officinalis protects keratinocytes from particulate matter-induced oxidative stress. Int J Med Sci 17: 63-70, 2020.
23. Kang KA, Piao MJ, Ryu YS, Hyun YJ, Park JE, Shilnikova K, Zhen AX, Kang HK, Koh YS, Jeong YJ and Hyun JW: Luteolin induces apoptotic cell death via antioxidant activity in human colon cancer cells. Int J Oncol 51: 1169-1178, 2017.
24. Cinelli G, Sbrocchi G, Iacovino S, Ambrosone L, Ceglie A, Lopez F and Cuomo F: Red wine-enriched olive oil emulsions: Role of wine polyphenols in the oxidative stability. Colloid Interfac 3: 59, 2019.
25. Herath HMUL, Piao MJ, Kang KA, Zhen AX, Fernando PDSM, Kang HK, Yi JM and Hyun JW: Hesperidin exhibits protective effects against PM2.5-mediated mitochondrial damage, cell cycle arrest, and cellular senescence in human HaCaT keratinocytes. Molecules 27: 4800, 2022.
26. Kang KA, Zhang R, Chae S, Lee SJ, Kim J, Kim J, Jeong J, Lee J, Shin T, Lee NH and Hyun JW: Phloroglucinol (1,3,5-trihydroxybenzene) protects against ionizing radiation-induced cell damage through inhibition of oxidative stress in vitro and in vivo. Chem Biol Interact 185: 215-226, 2010.
27. Dias MC, Pinto DCGA and Silva AMS: Plant flavonoids: Chemical characteristics and biological activity. Molecules 26: 5377, 2021.
28. Rudrapal M and Chetia D: Plant flavonoids as potential source of future antimalarial leads. Sys Rev Pharm 8: 13-18, 2017.
29. Ullah A, Munir S, Badshah SL, Khan N, Ghani L, Poulson BG, Emwas AH and Jaremko M: Important flavonoids and their role as a therapeutic agent. Molecules 25: 5243, 2020.
30. Kang KA, Zhang R, Piao MJ, Zhen AX, Herath HMUL, Fernando PDSM and Hyun JW: Luteolin triggered apoptosis in human colon cancer cells mediated by endoplasmic reticulum stress signaling. Food Suppl Biomater Health 2: e24, 2022.
31. Kang KA, Piao MJ, Hyun YJ, Zhen AX, Cho SJ, Ahn MJ, Yi JM and Hyun JW: Luteolin promotes apoptotic cell death via upregulation of Nrf2 expression by DNA demethylase and the interaction of Nrf2 with p53 in human colon cancer cells. Exp Mol Med 51: 1-14, 2019.
32. Park J, Kang KA, Zhang R, Piao MJ, Park S, Kim JS, Kang SS and Hyun JW: Antioxidant and cytotoxicity effects of luteolin. Toxicol Res 22: 391-395, 2006.
33. Liu YS, Yang Q, Li S, Luo L, Liu HY, Li XY and Gao ZN: Luteolin attenuates angiotensin II-induced renal damage in apolipoprotein E-deficient mice. Mol Med Rep 23: 157, 2021.
34. Boukhenouna S, Wilson MA, Bahmed K and Kosmider B: Reactive oxygen species in chronic obstructive pulmonary disease. Oxid Med Cell Longev 2018: 5730395, 2018.
35. Son B, Kwon T, Lee S, Han I, Kim W, Youn H and Youn B: CYP2E1 regulates the development of radiation-induced pulmonary fibrosis via ER stress-and ROS-dependent mechanisms. Am J Physiol Lung Cell Mol Physiol 313: L916-L929, 2017.
36. Su LJ, Zhang JH, Gomez H, Murugan R, Hong X, Xu D, Jiang F and Peng ZY: Reactive oxygen species-induced lipid peroxidation in apoptosis, autophagy, and ferroptosis. Oxid Med Cell Longev 2019: 5080843, 2019.
37. Lee JS, Kim YR, Song IG, Ha SJ, Kim YE, Baek NI and Hong EK: Cyanidin-3-glucoside isolated from mulberry fruit protects pancreatic β-cells against oxidative stress-induced apoptosis. Int J Mol Med 35: 405-412, 2015.
38. Upadhyay S, Vaish S and Dhiman M: Hydrogen peroxide-induced oxidative stress and its impact on innate immune responses in lung carcinoma A549 cells. Mol Cell Biochem 450: 135-147, 2019.
39. Campbell NK, Fitzgerald HK and Dunne A: Regulation of inflammation by the antioxidant haem oxygenase 1. Nat Rev Immunol 21: 411-425, 2021.
40. Park C, Lee H, Noh JS, Jin CY, Kim GY, Hyun JW, Leem SH and Choi YH: Hemistepsin a protects human keratinocytes against hydrogen peroxide-induced oxidative stress through activation of the Nrf2/HO-1 signaling pathway. Arch Biochem Biophys 691: 108512, 2020.
41. Hua W, Li S, Luo R, Wu X, Zhang Y, Liao Z, Song Y, Wang K, Zhao K, Yang S and Yang C: Icariin protects human nucleus pulposus cells from hydrogen peroxide-induced mitochondria-mediated apoptosis by activating nuclear factor erythroid 2-related factor 2. Biochim Biophys Acta Mol Basis Dis 1866: 165575, 2020.
42. Oh Y, Ahn CB, Nam KH, Kim YK, Yoon NY and Je JY: Amino acid composition, antioxidant, and cytoprotective effect of blue mussel (Mytilus edulis) hydrolysate through the inhibition of caspase-3 activation in oxidative stress-mediated endothelial cell injury. Mar Drugs 17: 135, 2019.
43. Kim EN, Lee HS and Jeong GS: Cudratricusxanthone O inhibits H_2O_2-induced cell damage by activating Nrf2/HO-1 pathway in human chondrocytes. Antioxidants (Basel) 9: 788, 2020.
44. Xia Y, Tan W, Yuan F, Lin M and Luo H: Luteolin attenuates oxidative stress and colonic hypermobility in water avoidance stress rats by activating the Nrf2 signaling pathway. Mol Nutr Food Res 68: e2300126, 2024.
45. Tan X, Yang Y, Xu J, Zhang P, Deng R, Mao Y, He J, Chen Y, Zhang Y, Ding J, *et al*: Luteolin exerts neuroprotection via modulation of the p62/Keap1/Nrf2 pathway in intracerebral hemorrhage. Front Pharmacol 10: 1551, 2020.
46. Rajput SA, Shaukat A, Wu K, Rajput IR, Baloch DM, Akhtar RW, Raza MA, Najda A, Rafał P, Albrakati A, *et al*: Luteolin alleviates aflatoxinB1-induced apoptosis and oxidative stress in the liver of mice through activation of Nrf2 signaling pathway. Antioxidants (Basel) 10: 1268, 2021.
47. Li L, Luo W, Qian Y, Zhu W, Qian J, Li J, Jin Y, Xu X and Liang G: Luteolin protects against diabetic cardiomyopathy by inhibiting NF-κB-mediated inflammation and activating the Nrf2-mediated antioxidant responses. Phytomedicine 59: 152774, 2019.
48. Mapuskar KA, Pulliam CF, Zepeda-Orozco D, Griffin BR, Furqan M, Spitz DR and Allen BG: Redox regulation of Nrf2 in cisplatin-induced kidney injury. Antioxidants (Basel) 12: 1728, 2023.